MMF1928 Project 3:
Stochastic Interest Rates and Swaptions

Ian Lee, Joshua Kim, Linlong Wu

December 21, 2022

Abstract

The aim of the report is to establish a mathematical framework to study stochastic interest rate models in finance, namely a two-factor Vasicek short rate model. This lays the analytical expression for a zero-coupon bond price, followed by numerical analyses with SDE discretization and Monte Carlo simulation to estimate the term structure. Furthermore it conducts parameter analysis of the Vasicek model and their roles in determining the yield curve. Lastly, the report studies an application of the model on swaptions and Black implied volatility of a swaption under log-normal swap rate model (LSM) and investigates how it changes as a function of strike.

Contents

1 Introduction

In finance, an interest rate is the amount charged per period as a proportion of the principal lent, deposited, or borrowed. While conceptually simple, it has broad applications in the financial markets, namely for valuation of interest rate derivatives. According to the Bank for International Settlements (BIS), the notional value of the interest rate derivatives market is estimated to be $502.59 trillion (in USD) as of June 2022, making it the largest derivatives market in the world [1]. Market participants utilize these rates products for numerous intentions, whether it being hedging or speculative. Regardless of the purpose, accurate pricing of interest rate derivative contracts is essential for an efficient and mature financial market due to their heavy usage in the industry.

Classical pricing models, such as Black-Scholes framework, assumes constant or deterministic interest rate for mathematical convenience and ease of computation. This, however, does not reflect the real world with unpredictable interest rates especially under the current economic state where central banks are rapidly raising their target rates in attempt to mitigate worldwide inflation. This calls for a need to implement a model that captures the stochastic nature of interest rates.

While there exist a wide range of stochastic short rate models, they can be categorized into two classes by the number of uncertainties in the model – *one-factor* and *two-factor* models. Specifically, the report focuses on a particular kind of two-factor models, i.e. two-factor *Vasicek model*. First introduced in 1977 by Oldrich Vasicek, it has been favored by practitioners for its simplicity and the mean reverting property.

In the report, the theoretical analysis presents an analytical formula for T-maturity bond price process under the two-factor Vasicek model accompanied with a deterministic process. This lays the mathematical foundation for the numerical analysis which investigates an alternative method to construct a yield curve by SDE discretization and Monte Carlo simulations. Furthermore, the paper analyzes how each parameter in the Vasicke model plays its role in determining the term structure using the analytical expression. It is followed by discussions on numerically pricing interest rate swaps and Black implied volatility under the log-normal swap rate model (LSM).

2 Model Setup

While the primary focus of the report in the two-factor Vasicek model, the one-factor counterpart is also discussed to facilitate the derivation under the two-factor model. This section introduces the model setups of both interest rate models.

2.1 One-Factor Vasicek Model

Suppose the short rate of interest in the economy $r = (r_t)_{t\geq 0}$ is modelled by the following SDE:

$$dr_t = \kappa(\theta - r_t)dt + \sigma dW_t \tag{1}$$

where $\kappa, \sigma > 0$ and θ are constant and W_t is the standard Brownian process under the risk-neutral measure $\mathbb{Q}$.

2.2 Two-Factor Vasicek Model

Suppose the short rate of interest in the economy is denoted as $r = (r_t)_{t\geq 0}$ and $r_t = \phi_t + x_t + y_t$, where x_t and y_t satisfy the following pair of SDEs:

$$\begin{aligned} dx_t &= -\alpha x_t dt + \sigma dW_t^1 \\ dy_t &= -\beta y_t dt + \eta dW_t^2 \end{aligned} \tag{2}$$

where $\alpha, \beta, \sigma, \eta > 0$ are constant, $W^{1,2} = (W_t^{1,2})_{t\geq 0}$ are independent standard Brownian processes under the risk-neutral measure $\mathbb{Q}$, and ϕ_t is a deterministic function of time.

For the rest of the report, the following function and model parameters are used unless specified otherwise:

$$\phi_t = a + b\left(\frac{1 - e^{-\lambda t}}{\lambda t} - e^{-\lambda t}\right), \qquad a = 2\%,\ b = 5\%,\ \lambda = 0.75$$

and

$$x_0 = -0.5\%,\ y_0 = 0.5\%,\ \alpha = 3,\ \beta = 1,\ \sigma = 1\%,\ \eta = 0.5\%$$

3 Analytical Analysis of Bond Price

3.1 One-Factor Vasicek Model

Consider a process $m = (m_t)_{t\geq 0}$ where $m_t = e^{\kappa t} r_t$. Using the Itô's lemma, the differential dm_t can be expressed as:

$$\begin{aligned} dm_t &= \kappa e^{\kappa t} r_t dt + e^{\kappa t} dr_t + d[e^{\kappa t}, r_t]_t \\ &= \kappa e^{\kappa t} r_t dt + e^{\kappa t}(\kappa(\theta - r_t)dt + \sigma dW_t) + 0 \\ &= \theta\kappa e^{\kappa t} dt + \sigma e^{\kappa t} dW_t \end{aligned}$$

By integrating both sides from time t to T, we obtain

$$\begin{aligned}
m_T - m_t &= \int_t^T \theta\kappa e^{\kappa u} du + \int_t^T \sigma e^{\kappa u} dW_u \\
e^{\kappa T} r_T - e^{\kappa t} r_t &= \int_t^T \theta\kappa e^{\kappa u} du + \sigma \int_t^T e^{\kappa u} dW_u \\
e^{\kappa T} r_T - e^{\kappa t} r_t &= \theta(e^{\kappa T} - e^{\kappa t}) + \sigma \int_t^T e^{\kappa u} dW_u \\
e^{\kappa T} r_T &= e^{\kappa t} r_t + \theta(e^{\kappa T} - e^{\kappa t}) + \sigma \int_t^T e^{\kappa u} dW_u \\
r_T &= e^{-\kappa(T-t)} r_t + \theta(1 - e^{-\kappa(T-t)}) + \sigma \int_t^T e^{-\kappa(T-u)} dW_u \\
r_T &= \theta + e^{-\kappa(T-t)}(r_t - \theta) + \sigma \int_t^T e^{-\kappa(T-u)} dW_u
\end{aligned} \tag{3}$$

Recall *Equation 1* and integrate both sides from time t to T to obtain $\int_t^T r_u du$.

$$\begin{aligned}
dr_t &= \kappa(\theta - r_t)dt + \sigma dW_t \\
r_T - r_t &= \kappa \int_t^T \theta du - \kappa \int_t^T r_u du + \sigma \int_t^T dW_u \\
\kappa \int_t^T r_u du &= -(r_T - r_t) + \kappa\theta(T-t) + \sigma \int_t^T dW_u \\
&= -(\theta + e^{-\kappa(T-t)}(r_t - \theta) + \sigma \int_t^T e^{-\kappa(T-u)} dW_u - r_t) \\
&\quad + \kappa\theta(T-t) + \sigma \int_t^T dW_u \\
&= -\theta - e^{-\kappa(T-t)}(r_t - \theta) - \sigma \int_t^T e^{-\kappa(T-u)} dW_u + r_t \\
&\quad + \kappa\theta(T-t) + \sigma \int_t^T dW_u \\
&= \kappa\theta(T-t) + (r_t - \theta)(1 - e^{-\kappa(T-t)}) + \sigma \int_t^T (1 - e^{-\kappa(T-u)}) dW_u \\
\int_t^T r_u du &= \theta(T-t) + (r_t - \theta)\frac{1 - e^{-\kappa(T-t)}}{\kappa} + \sigma \int_t^T \frac{1 - e^{-\kappa(T-u)}}{\kappa} dW_u
\end{aligned}$$

Let $\ell(t, T; \kappa) = \frac{1-e^{-\kappa(T-t)}}{\kappa}$. Then

$$\int_t^T r_u du = \theta(T-t) + (r_t - \theta)\ell(t, T; \kappa) + \sigma \int_t^T \ell(u, T; \kappa) dW_u \tag{4}$$

Hence by Itô's isometry, we obtain the following distribution under $\mathbb{Q}$:

$$\int_t^T r_u du \overset{\mathbb{Q}}{\sim} \mathcal{N}\left(\theta(T-t) + (r_t - \theta)\ell(t, T; \kappa),\ \sigma^2 \int_t^T \ell(u, T; \kappa)^2 du\right) \tag{5}$$

3.2 Two-Factor Vasicek Model

We directly proceed to determining the time integral of x_t and y_t respectively under the two-factor Vasicek model using *Equation 4* from *Section 3.1*.

$$\begin{aligned} \int_t^T x_u du &= \ell(t,T;\alpha)x_t + \sigma \int_t^T \ell(u,T;\alpha) dW_u^1 \\ \int_t^T y_u du &= \ell(t,T;\beta)x_t + \eta \int_t^T \ell(u,T;\beta) dW_u^2 \end{aligned} \tag{6}$$

where $\ell(t,T;\gamma) = \frac{1-e^{-\gamma(T-t)}}{\gamma}$ for a given parameter γ. The former integral is a special case of the one-factor model with $\kappa = \alpha,\ \theta = 0,\ \sigma = \sigma$ and the latter is with $\kappa = \beta,\ \theta = 0,\ \sigma = \eta$.

Similar to *Equation 7*, we can subsequently obtain the following distributions under $\mathbb{Q}$ using Itô's isometry:

$$\begin{aligned} \int_t^T x_u du &\overset{\mathbb{Q}}{\sim} \mathcal{N}\left(\ell(t,T;\alpha)x_t,\ \sigma^2 \int_t^T \ell(u,T;\alpha)^2 du\right) \\ \int_t^T y_u du &\overset{\mathbb{Q}}{\sim} \mathcal{N}\left(\ell(t,T;\beta)y_t,\ \eta^2 \int_t^T \ell(u,T;\beta)^2 du\right) \end{aligned} \tag{7}$$

We now state the *Fundamental Theorem of Asset Pricing* (FTAP), a crucial result often invoked when pricing derivatives.

Theorem 1 (Fundamental Theorem of Asset Pricing)**.** *An economy does not admit any arbitrage opportunities if and only if there exists:*

1. *a* ***numeraire*** *asset, i.e. a traded asset B satisfying $\mathbb{P}(B_t > 0) = 1$ for all t;*
2. *an associated probability measure $\mathbb{Q}^B$ equivalent to the physical measure $\mathbb{P}$,*

such that the prices of all traded assets relative to B are martingales under $\mathbb{Q}^B$, i.e. for any traded asset A we have:

$$\frac{A_t}{B_t} = \mathbb{E}^{\mathbb{Q}^B}\left[\frac{A_u}{B_u} \mid \mathcal{F}_t\right], \quad u > t \tag{8}$$

where $\mathcal{F}_t$ is the σ-algebra generated by all asset paths up to time t.

Suppose the economy has a risk-free asset (bank account) $B = (B_t)_{t\geq 0}$ and its price evolution is described as the following dynamics:

$$\begin{aligned} dB_t &= r_t B_t dt, \quad B_0 = 1 \\ \implies \quad B_t &= e^{-\int_t^T r_u du} \end{aligned} \tag{9}$$

Given that bonds are tradable assets in financial markets, we can determine the price process of a zero-coupon bond $P(T) = (P_t(T))_{t\in[0,T]}$ with maturity T and

principal value of $P_T(T) = 1$ by invoking the FTAP.

$$\begin{aligned} \frac{P_t(T)}{B_t} &= \mathbb{E}^{\mathbb{Q}}\left[\frac{P_T(T)}{B_T}\middle|\mathcal{F}_t\right] \\ P_t(T) &= \mathbb{E}^{\mathbb{Q}}\left[\frac{B_t}{B_T}\middle|\mathcal{F}_t\right] = \mathbb{E}^{\mathbb{Q}}\left[e^{-\int_t^T r_u du}\middle|\mathcal{F}_t\right] \end{aligned} \tag{10}$$

Using the fact that $\mathbb{E}[e^X] = e^{\mu+\frac{1}{2}\sigma^2}$ for any normally distributed random variable $X \sim \mathcal{N}(\mu, \sigma^2)$, we achieve the following result:

$$\begin{aligned} P_t(T) &= \mathbb{E}^{\mathbb{Q}}\left[e^{-\int_t^T r_u du}\middle|\mathcal{F}_t\right] \\ &= \mathbb{E}^{\mathbb{Q}}\left[e^{-\int_t^T (\phi_u + x_u + y_u) du}\middle|\mathcal{F}_t\right] \\ &= \left(e^{-\int_t^T \phi_u du}\right)\mathbb{E}^{\mathbb{Q}}\left[e^{-\int_t^T x_u du}\middle|\mathcal{F}_t\right]\mathbb{E}^{\mathbb{Q}}\left[e^{-\int_t^T y_u du}\middle|\mathcal{F}_t\right] \\ &= e^{-\int_t^T \phi_u du} \cdot e^{-\ell(t,T;\alpha)x_t + \frac{1}{2}\sigma^2\int_t^T \ell(u,T;\alpha)^2 du} \cdot e^{-\ell(t,T;\beta)y_t + \frac{1}{2}\eta^2\int_t^T \ell(u,T;\beta)^2 du} \\ &= e^{-\int_t^T \phi_u du + \frac{1}{2}\sigma^2\int_t^T \ell(u,T;\alpha)^2 du + \frac{1}{2}\eta^2\int_t^T \ell(u,T;\beta)^2 du - \ell(t,T;\alpha)x_t - \ell(t,T;\beta)y_t} \end{aligned}$$

Consequently, we arrive at an analytical formula for the bond price in an affine form as follows:

$$P_t(T) = e^{A_t(T) - B_t(T)x_t - C_t(T)y_t}$$

where

$$\begin{aligned} A_t(T) &= -\int_t^T \phi_u du + \frac{1}{2}\sigma^2\int_t^T \ell(u,T;\alpha)^2 du + \frac{1}{2}\eta^2\int_t^T \ell(u,T;\beta)^2 du \\ &= -\int_t^T \phi_u du + \sigma^2\left(\frac{2\alpha(T-t) + 4e^{-\alpha(T-t)} - e^{-2\alpha(T-t)} - 3}{4\alpha^3}\right) \\ &\quad + \eta^2\left(\frac{2\beta(T-t) + 4e^{-\beta(T-t)} - e^{-2\beta(T-t)} - 3}{4\beta^3}\right) \\ B_t(T) &= \ell(t,T;\alpha) = \frac{1 - e^{-\alpha(T-t)}}{\alpha} \\ C_t(T) &= \ell(t,T;\beta) = \frac{1 - e^{-\beta(T-t)}}{\beta} \end{aligned} \tag{11}$$

The following is how the time integral of $\ell(u,T;\gamma)^2$ has been computed:

$$\begin{aligned}
\int_t^T \ell(u,T;\gamma)^2 du &= \int_t^T \left(\frac{1-e^{-\gamma(T-u)}}{\gamma}\right)^2 du \\
&= \int_t^T \frac{1-2e^{-\gamma(T-u)}+e^{-2\gamma(T-u)}}{\gamma^2} du \\
&= \int_t^T \left(\frac{1}{\gamma^2} - \frac{2e^{-\gamma(T-u)}}{\gamma^2} + \frac{e^{-2\gamma(T-u)}}{\gamma^2}\right) du \\
&= \left(\frac{T-t}{\gamma^2} - \frac{2(1-e^{-\gamma(T-t)})}{\gamma^3} + \frac{1-e^{-2\gamma(T-u)}}{2\gamma^3}\right) \\
&= \left(\frac{2\gamma(T-t)}{2\gamma^3} - \frac{4(1-e^{-\gamma(T-t)})}{2\gamma^3} + \frac{1-e^{-2\gamma(T-u)}}{2\gamma^3}\right) \\
&= \left(\frac{2\gamma(T-t)-4e^{-\gamma(T-t)}-e^{-2\gamma(T-t)}-3}{2\gamma^3}\right)
\end{aligned}$$

4 Numerical Analysis

Modelling and pricing derivatives with stochastic dynamics can often be challenging as closed-form solutions of the underlying SDEs may be unknown. Typically, one circumvents the problem by resorting to numerical approximations under some computational frameworks. Fortunately for this project, the price of a T-maturity bond has an analytical expression as shown in *Section 3*. This section adopts a Monte Carlo approach by discretizing the interest rate SDEs to estimate the bond yield curve, which is then compared to the analytical formula to demonstrate the effectiveness of the numerical solution. Furthermore the section investigates what role the parameters in the interest rate SDEs play in determining the term structure.

4.1 Interest Rate SDE Discretization

Suppose one wishes to simulate values from the SDEs expressed as *Equation 2* without knowing their distributions. In this event we can simulate a *discretizd* version of the SDEs, i.e. a discretized process $\hat{x} = \{\hat{x}_0, \hat{x}_1, \ldots, \hat{x}_n\}$ and $\hat{y} = \{\hat{y}_0, \hat{y}_1, \ldots, \hat{y}_n\}$, at the expense of computational effort. While there are a number of discretization schemes available, the simplest and most common scheme is the *Euler* scheme as it is intuitive and easy to implement.

For the purpose of this project, the Euler scheme would satisfy:

$$\hat{x}_{t+\Delta t} - \hat{x}_t = -\alpha \hat{x}_t \Delta t + \sigma \sqrt{\Delta t} Z_t^1, \quad \hat{x}_0 = x_0$$
$$\hat{y}_{t+\Delta t} - \hat{y}_t = -\beta \hat{y}_t \Delta t + \eta \sqrt{\Delta t} Z_t^2, \quad \hat{y}_0 = y_0$$

Under the assumption that a year consists of 252 trading days, we generated 1,000 simulations of risk-neutral interest rate paths – x_t, y_t, and r_t – out to 10 years with discretization of 1 step per day. As the two factors x_t and y_t both contribute to the stochasticity of the short rate process r_t, we investigate them along with the interest rate. In general, we observed that both the risk-neutral interest rate r_t and its components x_t and y_t exhibit mean-reverting behavior.

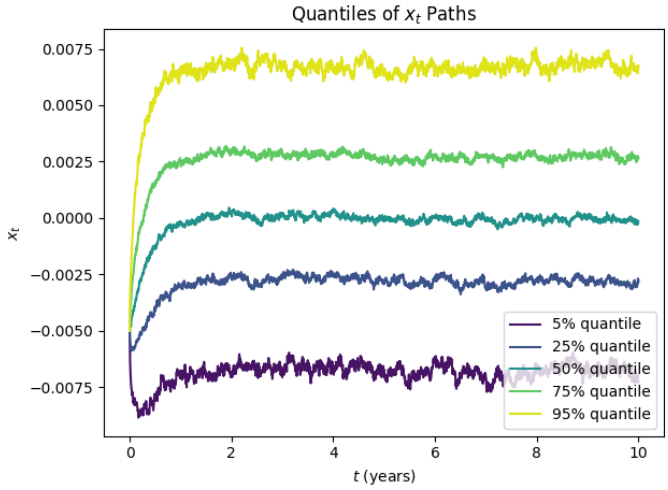

Figure 1: *quantiles of x_t paths based on 10000 simulations from SDE discretization using the Euler scheme*

Figure 1 illustrates the simulated paths of x_t and their five quantiles. One can observe the process reverts to its mean of 0 within a year at the 50% quantile and continues to fluctuate closely around the mean. This pattern is portrayed across all quantiles in an ascending manner, with the highest 95% quantile and the lowest 5% quantile bouncing around 0.0075 and -0.0075 respectively.

Switching to the paths of y_t, we discovered a descending mean-reversion trend as illustrated in *Figure 2*. While the 50% quantile also arrives at zero in two years, it is worth noticing that the pace at which it reverts to the mean is slower than that of the x_t process. Moreover, the quantile bands appear to be narrower, where the 95% quantile and the 5% quantile bounce around 0.006 and -0.006 respectively.

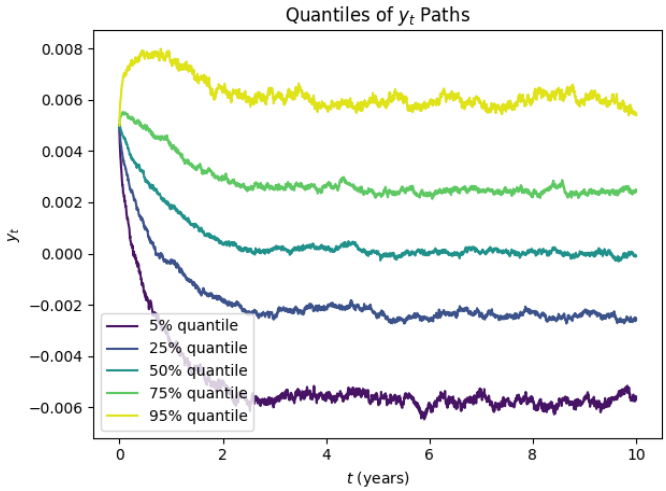

Figure 2: *quantiles of y_t paths based on 10000 simulations from SDE discretization using the Euler scheme*

The logic behind these phenomena traces back to the SDEs for both processes. Recall from the SDEs expressed as *Equation 2* – the value of the speed coefficient α for the process x_t is greater than that of β for the process y_t, resulting in a faster rate of mean-reversion. Additionally, the difference between diffusion coefficients σ and η accounts for the unmatched inter-quantile bandwidths.

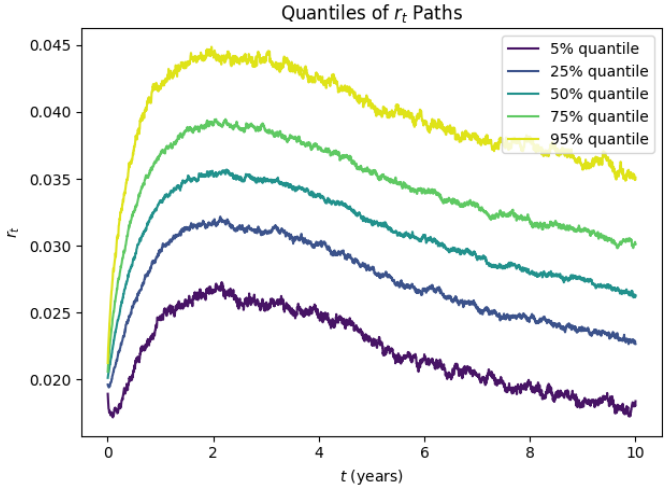

Figure 3: *quantiles of r_t paths based on 10000 simulations from SDE discretization using the Euler scheme*

Lastly, *Figure 3* illustrates the simulated paths of the short rate r_t. Confirming with the above analyses, we witnessed movements divided into two regimes. The paths surge up in the first two years and then drop monotonically, converging towards the mean of ϕ_t.

4.2 Bond Yield Monte Carlo Estimation

Having seen the dynamics of the stochastic interest rates, we are interested in investigating the term structure of the bond. The term structure, often depicted as a yield curve, portrays how the yields of fixed-income instruments, such as bonds, vary as a function of their time remaining to maturity. Two approaches have been employed – numerical and analytical.

We first performed 10,000 runs of Monte Carlo simulation to obtain the estimates of the short rate process r_t. Leveraging *Equation 10*, the zero-coupon bond price at time $t = 0$ for various maturity dates T can be determined as a form of an expectation.

$$P_0(T) = \mathbb{E}^{\mathbb{Q}}\left[e^{-\int_0^T r_u d_u}\right] = e^{-YT} \tag{12}$$

where Y denotes the bond yield. The integral $\int_0^T r_u d_u$ can be computed numerically as a Riemann sum as follows:

$$\int_0^T r_u d_u \approx \sum_{i=1}^{n} \hat{r}_i \Delta t_i \tag{13}$$

where $\hat{r}$ is the discretized short rate process and Δt is the size of each time step. The analytical approach directly utilizes the result obtained from *Equation 11*. At time $t = 0$, the bond price is:

$$P_0(T) = e^{A_0(T) - B_0(T)x_0 - C_0(T)y_0} = e^{-YT}. \tag{14}$$

Each method produces an estimate for the bond price, from which we could calculate the yield Y at each maturity date T, ranging from one month to 10 years in steps of one month.

$$Y = -\frac{ln\ (P_0 T)}{T}$$

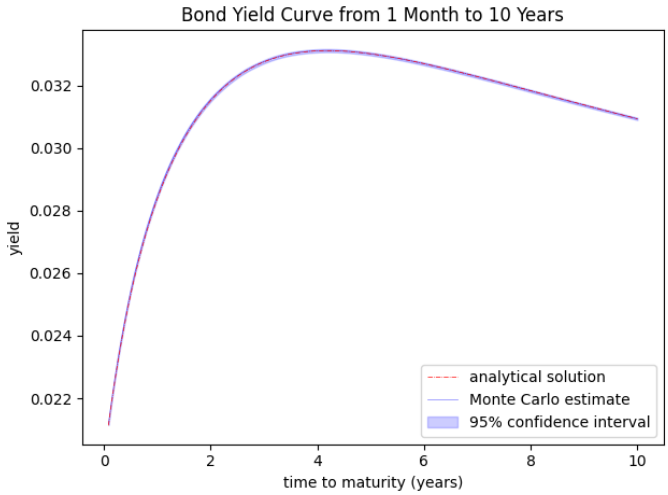

Figure 4: *analytical solution and Monte Carlo estimate with 95% confidence interval of the bond yield curve for maturities ranging from one month to ten years in steps of one month*

Figure 4 presents the yield curves of both approaches, along with a 95% confidence interval of the numerical result. This validates our analytical representation of the bond price process as it is evident from the plot that the two curves closely overlap each other. Additionally, the accuracy of the numerical simulations is confirmed as the confidence band is very narrow, tightly containing both curves.

Taking a closer look at the term structure, we see that bond yield first increases along with maturity, reaching its peak at a maturity of 4 years, then declining continuously. Intuitively when one extends the time to maturity, which can be interpreted as the duration for a zero-coupon bond, investors bear higher level of risks. These risks originate from potential defaults, liquidity risk and sensitivity to changes in interest rates. As a result, the premium to compensate for the risks increases, which is described by the rising bond yields. In our simulated environment, however, the interest rate reverts back towards its mean at longer maturities. Consequentially, we observe the bond yield declining from its maximum as we travel along the axis of maturities.

4.3 Parameter Analysis

The above analyses are conducted using the base set of parameter values. To grasp a better understanding of how each parameter impacts the term structure, this section carries out parameter analyses.

4.3.1 Changing Speed Coefficients

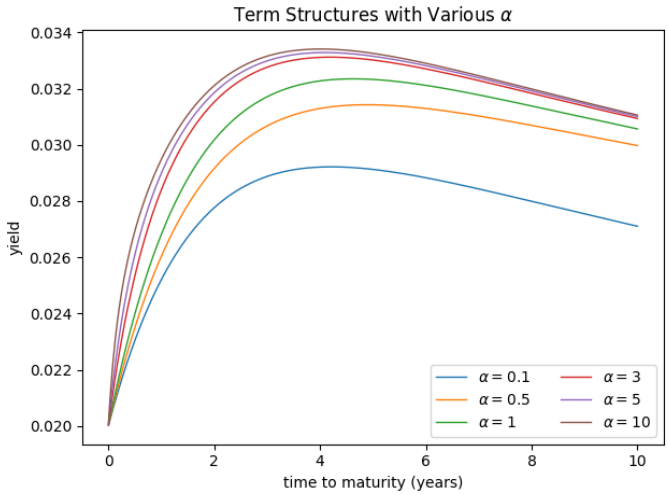

Figure 5: *term structure plots using the analytical solution with various values of α*

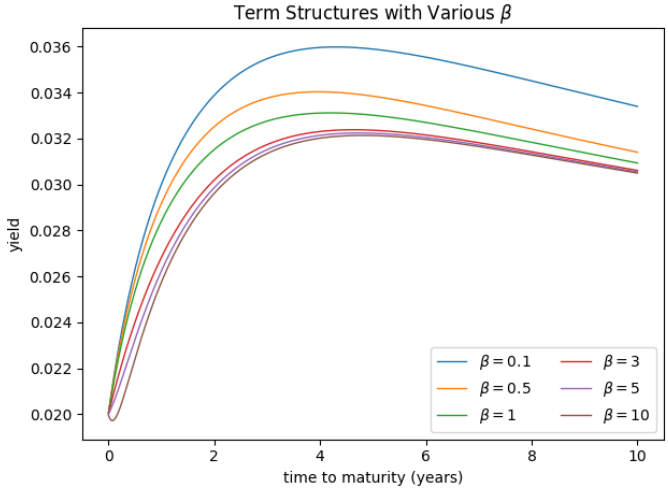

Figure 6: *term structure plots using the analytical solution with various values of β*

As α increases, *Figure 5* portrays that the yield converges closer to the term structure solely influenced by the deterministic function ϕ_t. Moreover, when α is small (i.e. $\alpha < 3$), a small change of the parameter causes a significant increase in the yield over time. For instance, when α changes from 0.1 to 0.5,

the yield rapidly increases over time, but once α is greater than 3, the changes are minimal.

As β controls the speed at which the y_t process mean-reverts, we obserse that the yield curve converging at a faster rate towards the deterministic structure, as shown in *Figure 6*, when passed with larger values of β. In addition, a larger β value results in a lower yield curve. The marginal effect that a varying β yields, however, diminishes in a similar fashion as we witnessed for α.

4.3.2 Changing Volatility Coefficients

Under the two-factor Vasicek model, σ and η mark the diffusion level in x_t and y_t processes. Expanding the magnitude of these two terms would introduce additional volatility to our interest rate process, the impact of which trickles down to the yield curve.

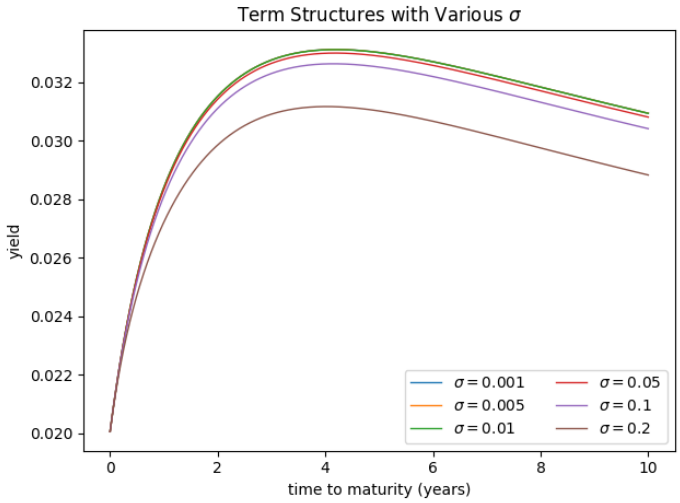

Figure 7: *term structure plots using the analytical solution with various values of* σ

The changes of σ leaves a noticeable impact on the yield as shown in *Figure 7*. Generally, larger values of σ causes lower values of the yield. This is because given a more volatile process, the interest rate become more diffusive from the drift term. In consequence, the yield more likely moves lower when the volatility increases.

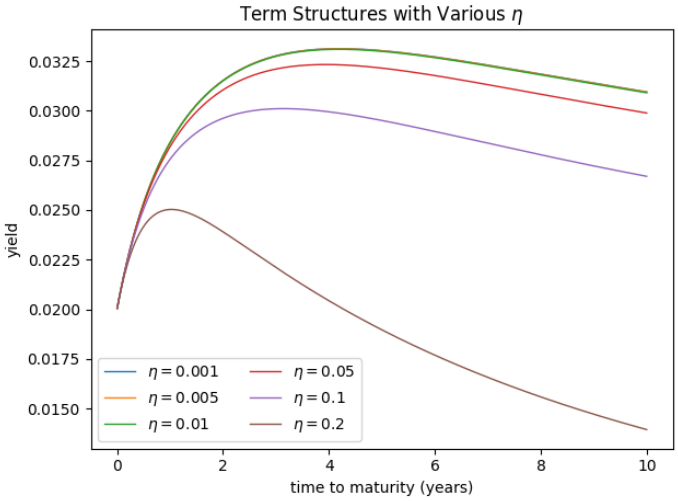

Figure 8: *term structure plots using the analytical solution with various values of η*

Similarly the impact of η on the yield curve expresses a similar pattern. The noticeable difference in the effect of η is much stronger compared to σ as shown in *Figure 8*. In particular, when $\eta > 0.05$, the yield begins to decrease at a much faster rate.

5 Swaption and Black Implied Volatility

This section discusses a particular type of interest rate derivatives products, *swaption*. As the name suggests, a swaption is an option written on an interest rate swap (IRS), i.e. it gives the holder the right but not an obligation to enter into a payer/receiver leg of a swap contract at a future date T, for a specified fixed rate F, and a specified tenure structure $\{\tau_0, \tau_1, ..., \tau_n\}$, where $\tau_0 \geq T$.

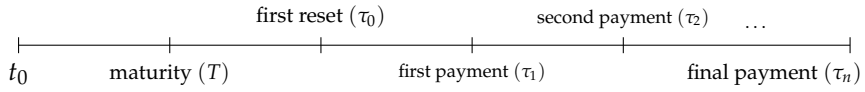

For the purpose of demonstration, we seek to investigate the dynamics of an IRS following a tenure structure $\{3, 3.25, \ldots, 6\}$, with the first reset date and maturity date set at 3 and the interval size between each payment being 0.25.

The realization of our analysis comes in two-fold: deriving the swap rate S_t and determining the Black implied volatility. Standing at today t_0, we make an assumption that the strike price of the swaption F is equal today's swap rate S_0. We then derive the Black implied volatility of the swaption, leveraging the log-normal swap rate model(LSM).

5.1 Swap Rate Derivation

The value of the fixed leg at time t can be written as:

$$v_t^{fixed} = \sum_{k=1}^{n} S_t N \triangle \tau_k P_t(\tau_k). \tag{15}$$

Similarly, it can be shown that the value of the floating leg at time t can be expressed as:

$$v_t^{float} = [P_t(\tau_0) - P_t(\tau_k)]N. \tag{16}$$

Swap rate S_t at time t is a fixed rate F such that the values of the floating and fixed leg match, i.e.

$$\begin{aligned} v_t^{fixed} &= v_t^{float} \\ \sum_{k=1}^{n} S_t N \Delta \tau_k P_t(\tau_k) &= [P_t(\tau_0) - P_t(\tau_k)]N \\ \implies \quad S_t &= \frac{P_t(\tau_0) - P_t(\tau_n)}{\sum_{k=1}^{n} \Delta \tau_k P_t(\tau_k)} \end{aligned} \tag{17}$$

5.2 Black Implied Volatility Derivation

The payoff of a swaption is:

$$v_T = (S_T - F)_+ \sum_{k=1}^{n} P_T(\tau_k)\Delta\tau_k = \mathcal{A}_T(S_T - F)_+ \tag{18}$$

where $\mathcal{A}_t = \sum_{k=1}^{n} P_t(\tau_k)\Delta\tau_k$ is the value of the annuity at time t. Invoking the FTAP with the annuity $\mathcal{A}_t$ as the numeraire, we obtain the price process of the swaption:

$$\begin{aligned} \frac{v_t}{A_t} &= \mathbb{E}_t^{\mathbb{Q}_\mathcal{A}} = \left[\frac{(S_T - F)_+ A_T}{A_T}\right] \\ v_t &= A_t \, \mathbb{E}_t^{\mathbb{Q}_\mathcal{A}}[(S_T - F)_+] \end{aligned} \tag{19}$$

Given that the swap rate process S_t is a martingale under the risk-neutral measure induced by the annuity $\mathbb{Q}_\mathcal{A}$, it must satisfy the following SDE:

$$dS_t = \delta_t S_t dW_t^\mathcal{A} \tag{20}$$

where $W_t^\mathcal{A}$ is the standard Brownian process under the measure $\mathbb{Q}_\mathcal{A}$. The log-normal swap rate model (LSM) assumes δ_t to be a constant. As a result, *Equation 20* resembles a geometric Brownian motion and the swap rate S_T can be expressed as:

$$S_T = S_t e^{-\frac{1}{2}\delta^2(T-t) + \delta(W_T^\mathcal{A} - W_t^A)} \tag{21}$$

Adopting the result from Black-Scholes framework given that the underlying behaves like a geometric Brownian motion, the value of the swaption is:

$$v_t = \mathcal{A}_t[S_t\Phi(d_+) - F\Phi(d_-)] \tag{22}$$

where $d_\pm = \frac{ln(\frac{S_t}{F}) \pm \frac{1}{2}\delta^2(T-t)}{\delta\sqrt{T-t}}$

The *Black implied volatility* of a swaption is δ_{imp} such that the value of the swaption v_t derived under the LSM is equal to the market price of the derivative.

5.3 Numerical Analysis

For the report, we obtain the market price of the swaption using the Monte Carlo simulations from the discretized interest rate SDEs. The numerical market price has been implemented under the risk-neutral measure $\mathbb{Q}$ as follows:

$$v_t = \mathbb{E}^{\mathbb{Q}}\left[e^{-\int_t^T r_u du}\mathcal{A}_T(S_T - F)_+\right]$$

where the integral $\int_t^T r_u du$ is computed as a Riemann sum.

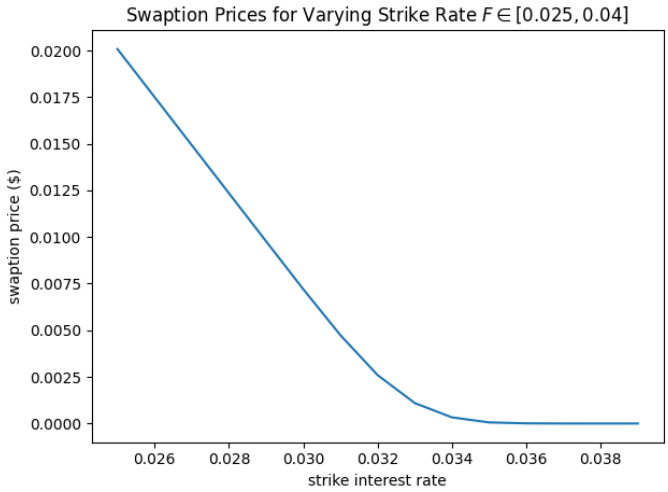

Figure 9: *plot of swaption prices calculated using 1000 paths generated with Monte Carlo simulations for varying strike price* $F \in [0.025, 0.04]$

Figure 9 demonstrates that the price of the swaption declines monotonically as the strike increases. The "elbow" of the curve is most evident around the strike rate of 0.0328, which is today's swap rate. At $F = 0.0328$, the Black implied volatility is $\delta imp = 0.0225$.

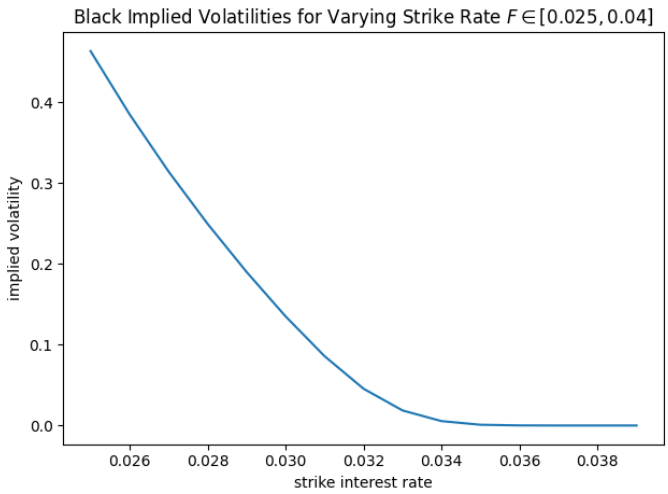

Figure 10: *plot of Black implied volatilities calibrated with numerically determined swaption prices for varying strike price* $F \in [0.025, 0.04]$

Not surprisingly, *Figure 10* illustrates that the implied volatility curve follows a similar pattern to that of the swaption price, exhibiting the well-known behavior of "volatility smirk". This phenomenon is commonly described by the term "crash–o–phobia", where investors are willing to pay more for protection of downside movement of the interest rate.

6 Conclusion

In this report, we begin by reviewing the Vasicek Model in one-factor setting, followed by the two-factor counterpart, extending the scope to incorporate an additional stochastic factor in modelling the short rate of interest in the economy. Leveraging the nature of the affine model, we derived an analytical solution to the T-maturity bond yield. The accuracy of this approach is validated by the comparison to the numerical result using Monte Carlo simulations and its 95% confidence interval. After investigating the dynamics of the interest rate process, we tuned various model parameters and tested their impacts on the term structure. For instance, changing the speed coefficients α and β can result in higher yield over time. We also detected a negative relationship between the yield and the diffusion coefficients σ and η.

Interest rate swaps and swaptions are two classes of interest rate derivatives we explored in the report. In particular, Black implied volatility was studied under the log-normal swap rate model (LSM). Equating the swaption price derived from the LSM model to the simulated market price, we obtained the implied volatility of 0.0225 under today's swap rate 0.0328. Varying the strike interest

rate, we appreciated the shape of the yield curve that exhibits characteristics of a "volatility smirk" with an elbow at today's swap rate.

To conclude, a well constructed interest rate model is crucial in capturing the stochastic nature of the market dynamics. It can justify many financial and economical arguments, and serve as a stepping stone for the valuation of financial instruments.

References

[1] "OTC derivatives statistics at end-December 2021," The Bank for International Settlements, 12-May-2022. [Online]. Available: www.bis.org. [Accessed: 18-Oct-2022].